


Indoxyl Sulfate and p-Cresyl Sulfate Promote Vascular Calcification and Associate with Glucose Intolerance

Britt Opdebeeck ¹, Stuart Maudsley,^{2,3} Abdelkrim Azmi,³ Annelies De Maré,¹ Wout De Leger,⁴ Bjorn Meijers,^{5,6} Anja Verhulst,¹ Pieter Evenepoel,^{5,6} Patrick C. D'Haese,¹ and Ellen Neven¹

¹Laboratory of Pathophysiology, Department of Biomedical Sciences, ²Receptor Biology Lab, Department of Biomedical Sciences, and ³Translational Neurobiology Group, Flanders Institute of Biotechnology Center for Molecular Neurology, Department of Biomedical Sciences, University of Antwerp, Antwerp, Belgium; ⁴Division of Molecular Design and Synthesis, Department of Chemistry and ⁶Laboratory of Nephrology, Department of Immunology and Microbiology, Catholic University of Leuven, Leuven, Belgium; and ⁵Division of Internal Medicine, Nephrology, University Hospitals Leuven, Leuven, Belgium

ABSTRACT

Background Protein-bound uremic toxins indoxyl sulfate (IS) and p-cresyl sulfate (PCS) have been associated with cardiovascular morbidity and mortality in patients with CKD. However, direct evidence for a role of these toxins in CKD-related vascular calcification has not been reported.

Methods To study early and late vascular alterations by toxin exposure, we exposed CKD rats to vehicle, IS (150 mg/kg per day), or PCS (150 mg/kg per day) for either 4 days (short-term exposure) or 7 weeks (long-term exposure). We also performed unbiased proteomic analyses of arterial samples coupled to functional bioinformatic annotation analyses to investigate molecular signaling events associated with toxin-mediated arterial calcification.

Results Long-term exposure to either toxin at serum levels similar to those experienced by patients with CKD significantly increased calcification in the aorta and peripheral arteries. Our analyses revealed an association between calcification events, acute-phase response signaling, and coagulation and glucometabolic signaling pathways, whereas escape from toxin-induced calcification was linked with liver X receptors and farnesoid X/liver X receptor signaling pathways. Additional metabolic linkage to these pathways revealed that IS and PCS exposure engendered a prodiabetic state evidenced by elevated resting glucose and reduced GLUT1 expression. Short-term exposure to IS and PCS (before calcification had been established) showed activation of inflammation and coagulation signaling pathways in the aorta, demonstrating that these signaling pathways are causally implicated in toxin-induced arterial calcification.

Conclusions In CKD, both IS and PCS directly promote vascular calcification *via* activation of inflammation and coagulation pathways and were strongly associated with impaired glucose homeostasis.

J Am Soc Nephrol 30: 751–766, 2019. doi: <https://doi.org/10.1681/ASN.2018060609>

Vascular calcification refers to the pathologic deposition of calcium-phosphate crystals in the arterial wall. This pathologic event represents a major clinical issue, because it significantly contributes to the high cardiovascular morbidity and mortality observed in patients with CKD.^{1–3} Except for phosphate and inflammation, other uremia-related factors may contribute to vascular calcification in patients with CKD. Among uremic retention solutes, indoxyl sulfate (IS)

Received June 12, 2018. Accepted February 13, 2019.

Published online ahead of print. Publication date available at www.jasn.org.

Correspondence: Dr. Patrick C. D'Haese, Laboratory of Pathophysiology, University of Antwerp, Campus Drie Eiken, Universiteitsplein 1, B-2610 Wilrijk, Belgium. Email: Patrick.dhaese@uantwerpen.be

Copyright © 2019 by the American Society of Nephrology

and p-cresyl sulfate (PCS) have been associated with cardiovascular disease and mortality.^{4–6} Both uremic toxins originate from protein fermentation in the intestine and accumulate in patients with CKD due to impaired renal clearance and increased intestinal production. p-Cresol and indole are generated by the intestinal microbial breakdown of tyrosine/phenylalanine and tryptophan, respectively. After intestinal absorption, these solutes undergo phase 2 reactions, predominantly by conjugation with sulfate.^{7,8} *In vitro* experiments have demonstrated that both uremic toxins can induce endothelial dysfunction.^{9–11} IS also induces vascular smooth muscle cell proliferation and upregulation of bone-specific proteins in these cells,^{12,13} which is a hallmark of the calcification process in the vessel wall.¹⁴ These results were further supported by the work by Adijiang *et al.*,¹⁵ which reported that exposure of hypertensive rats to IS promotes aortic calcification with the expression of bone-specific markers, such as *runx2*, alkaline phosphatase, and osteopontin.¹⁵ Additionally, treatment with AST-120, an oral spherical activated carbon adsorbent that reduces the serum concentrations of uremic toxins by limiting the intestinal absorption of generated microbial metabolites, went along with beneficial effects on the cardiovascular system, including attenuation of cardiac hypertrophy and fibrosis^{11,16} and a decline in vascular stiffness¹⁷ as well as reduced aortic calcification in predialysis patients with CKD.¹⁸ These findings suggest that protein-bound uremic retention solutes, which are only poorly cleared by conventional dialysis, may play an important role in vascular calcification, and thus, they may contribute to the high cardiovascular disease burden in patients with end stage renal failure. However, a recent clinical study found no association of predialysis total PCS and IS with cardiac death, sudden cardiac death, and first cardiovascular event.¹⁹ As commented by Evenepoel *et al.*,²⁰ these conflicting results point out that it is still unclear whether these uremic toxins are harmful to the vasculature. As such, experimental studies are required to explore the role of these uremic retention solutes in CKD-related vascular complications. Here, we aim to provide evidence for an etiologic role for IS and PCS as major contributors to the onset and development of calcification in the vessel wall of patients with CKD by use of a CKD rat model. Using a high-dimensionality unbiased proteomic approach, we have also investigated the potential complex molecular signaling events associated with toxin-mediated arterial calcification.

METHODS

Animal Experiments

All animal experiments were performed in accordance with the National Institutes of Health Guide for the Care and Use of Laboratory Animals 85–23 (1996) and approved by the University of Antwerp Ethics Committee (permit number 2012–13). Animals were housed two per cage, exposed to 12-hour light/dark cycles, and had *ad libitum* access to food and water.

Significance Statement

Vascular calcification contributes to high cardiovascular mortality in patients with CKD. Although research findings have suggested an association between the uremic toxins indoxyl sulfate and p-cresyl sulfate and cardiovascular disease, direct evidence has been lacking. In this study, the authors demonstrate in a rat model of CKD that continuous exposure to indoxyl sulfate or p-cresyl sulfate promotes moderate to severe calcification in the aorta and peripheral vessels. Activation of inflammation and coagulation pathways in the arterial wall plays a pivotal role in toxin-induced calcification and strongly associates with hyperglycemia and insulin resistance. These findings provide etiologic evidence for indoxyl sulfate and p-cresyl sulfate as major contributors to vascular calcification and suggest new avenues for identifying novel therapeutic targets to prevent or treat calcification in the vessel wall of patients with CKD.

Animal Study #1

To induce CKD, 42 male Wistar rats (225–250 g; Iffa Credo, Brussels, Belgium) were exposed to a 10-day adenine sulfate (Acros, Geel, Belgium) treatment *via* daily oral gavage (600 mg/kg per day). CKD rats fed a phosphate-enriched diet (1.2% Pi and 1.06% Ca; SSNIFF Spezialdiäten, Soest, Germany) were randomly assigned to three treatment groups: (1) vehicle ($n=14$), (2) 150 mg/kg IS (IS potassium salt; Sigma-Aldrich, St. Louis, MO; $n=14$), or (3) 150 mg/kg PCS (Department of Chemistry, KU Leuven, Leuven, Belgium; $n=14$). From the start of CKD induction onward until week 2, either IS or PCS was administered *via* the drinking water, which contained either of these toxins at a concentration corresponding to a daily intake of 150 mg/kg, followed by daily oral gavage of vehicle, IS (150 mg/kg), or PCS (150 mg/kg) from week 3 onward until euthanasia at week 7. Before the start of the study, at week 5, and at euthanasia, animals were placed in metabolic cages to collect 24-hour urine samples followed by blood sampling. At week 3, blood sampling was also performed. To enable measurement of dynamic bone parameters, all animals were labeled with tetracycline (30 mg/kg intravenously) 7 days before euthanasia and demeclocycline (25 mg/kg intravenously) 3 days before euthanasia.

Mortality was noted in the three study groups due to CKD; however, exposure to IS and particularly, PCS led to substantially higher mortality rates during the course of the study. Before the planned euthanasia, four vehicle-, six IS-, and eight PCS-exposed CKD rats died. Despite this increased mortality rate, our experimental animal cohorts remained sufficiently large to conclude our protocols effectively.

Animal Study #2

To explore early molecular changes in the arterial wall caused by the toxins IS and PCS before effective induction of vascular injury and calcification, an additional study was performed including animals that were exposed to these toxins for 4 days. To induce CKD, 12 male Wistar rats were exposed to adenine sulfate *via* daily oral gavage (600 mg/kg per day) for 4 days. CKD rats were fed a phosphate-enriched diet (1.2% Pi and 1.06% Ca), and they were randomly assigned to three

treatment groups: (1) vehicle ($n=4$), (2) 150 mg/kg IS ($n=4$), or (3) 150 mg/kg PCS ($n=4$) administered *via* the drinking water until euthanasia at day 4.

At euthanasia, rats of both animal studies were exsanguinated through the retro-orbital plexus after anesthesia with 60 mg/kg sodium pentobarbital (Nembutal; Ceva Santé Animale) *via* intraperitoneal injection.

Analyses of Biochemical Parameters

To assess renal function, creatinine was measured in serum and urine samples according to the Jaffé method. Total serum and urine phosphorus levels were analyzed with the Ecoline S Phosphate kit (Diasys, Holzheim, Germany), and serum and urinary calcium levels were determined with flame atomic absorption spectrometry (Perkin-Elmer, Wellesley, MA) after appropriate dilution in 0.1% $\text{La}(\text{NO}_3)_3$ to eliminate chemical interference. Serum immunoreactive parathyroid hormone (PTH) levels were measured using ELISA (Immutopics, San Clemente, CA). Serum IS and PCS levels were determined by liquid chromatography-tandem mass spectrometry (MS). Before the start of the study and at euthanasia, blood glucose levels were measured using the GlucoMen Lx Plus+ automated whole-blood glucometer.

Quantification of Adenine Crystals in the Kidney

At euthanasia, one slice of the left kidney was fixed in neutral buffered formalin for 4 hours and embedded in a paraffin block. Four-micrometer sections were stained with periodic acid–Schiff to quantify renal adenine crystals. The percentage of the area covered by adenine crystals was determined using Axiovision image analysis software (Release 4.5; Carl Zeiss, Oberkochen, Germany) by calculating the ratio of the number of pixels taken by the crystals to the number of pixels taken by the total renal tissue.

Analyses of Vascular Calcification

Vascular calcification was analyzed histomorphometrically on Von Kossa–stained sections. At euthanasia, the thoracic aorta was fixed in neutral buffered formalin for 90 minutes and cut into sections of 2–3 mm. These sections were embedded upright in a paraffin block, and 4- μm sections were stained for calcification with the Von Kossa method and counterstained with hematoxylin and eosin. The percentage calcified area was calculated using Axiovision image analysis software (Release 4.5), in which two color separation thresholds measure the total tissue area and the Von Kossa–positive area. After summing both absolute areas, the percentage of calcified area was calculated as the ratio of the Von Kossa–positive area to the total tissue area. Calcification in the aorta and smaller arteries was also quantified by calcium bulk analysis. For the purpose of this, the proximal section of the abdominal aorta and the left carotid and femoral arteries were isolated and directly weighed on a precision balance. The arterial samples were digested in 65% HNO_3 at 60°C overnight, after which the calcium content (milligrams of calcium per gram wet tissue)

of each artery was measured in the digestion liquid with flame atomic absorption spectrometry.

Analyses of Bone Parameters

At euthanasia, the left tibia was fixed in 70% ethanol overnight at 4°C, dehydrated, and embedded in 100% methylmethacrylate (Merck, Hohenbrunn, Germany) for bone histomorphometry. For analysis of the static bone parameters, 5- μm sections of the left tibia were Goldner stained for histomorphometric analysis of the proximal metaphysis with AxioVision Release 4.5 software. By using the formulas of Parfitt,²¹ the following static bone parameters were obtained: bone area and mineralized area on total tissue area, osteoid width, osteoid area on total bone area, osteoid perimeter, eroded perimeter, osteoblast perimeter, and osteoclast perimeter on total bone perimeter. For the analysis of dynamic bone parameters, tetracycline labels were visualized on 10- μm unstained tibia sections with fluorescence microscopy, and the length and distance between both labels were measured, enabling us to calculate additional dynamic bone parameters according to Dempster and colleagues.²¹

MS and Quantitative Proteomics of Aortic Samples

To elucidate the molecular signaling pathways responsible for the toxin-induced calcification in the aorta, an unbiased quantitative proteomic approach using iTRAQ (isobaric mass tag labeling for relative and absolute quantitation) labeling and MS was applied to simultaneously identify and quantify the proteins that are differentially up- or downregulated in aortic samples of CKD animals exposed to IS ($n=5$ for animal study #1; $n=3$ for animal study #2) or PCS ($n=5$ for animal study #1; $n=3$ for animal study #2) versus vehicle ($n=4$ for animal study #1; $n=3$ for animal study #2). The aorta samples were ground completely in the protein extraction buffer (8 M urea, 2 M thiourea, and 0.1% SDS in 50 mM triethylammonium bicarbonate solution). The concentrations of the proteins extracted from the aorta were quantified using the RCDC kit (Bio-Rad, Hercules, CA). Equal amounts of proteins from each sample were reduced and alkylated by tris-2-carboxyethyl phosphine and 5-methylmethanethiosulfate, respectively, before trypsin digestion. The resulting peptides from each sample were labeled using iTRAQ reagents (Sciex, Framingham, MA) following the manufacturer's instructions. To improve LC-MS/MS proteome coverage, samples were subjected to a 2D-LC fractionation system (Dionex ULTIMATE 3000; ThermoScientific, Waltham, MA). The mixed peptides were first fractionated on a strong cationic exchange chromatography polysulfoethyl aspartamide column (1 \times 150 mm; Dionex) and then, separated on a nano-LC C18 column (200 Å, 2 μm , 75 $\mu\text{m}\times$ 25 cm; Dionex). The nano-LC is coupled online to a QExact-Plus Orbitrap (ThermoScientific) mass spectrometer. The nano-LC eluents were infused to the Orbitrap mass spectrometer with a capillary at 1.7 kV on a nano-ESI source at a flow rate of 300 nl/min.

Data-dependent acquisition in positive ion mode was performed for a selected mass range of 350–1800 m/z at MS1 level (140,000 resolution) and MS2 level (17,500 resolution). The raw data were analyzed by Proteome Discoverer 2.1 Software (ThermoScientific) using Sequest HT as the search engine against the *Rattus norvegicus* (UP000002494) UniProt/SwissProt database (2017) with threshold of confidence above 99% (false discovery rate <1%). The list of identified proteins containing iTRAQ ratios of expression levels over control samples was generated. The MS proteomics data have been deposited in the ProteomeXchange Consortium via the PRIDE²² partner repository with the dataset identifier PXD012582.

Bioinformatic Analyses

Proteins identified according to the statistical MS cutoffs described previously were then subsequently used for additional bioinformatics analyses. To identify the significantly altered proteins (*i.e.*, proteins differentially expressed due to IS and PCS exposure compared with vehicle exposure), raw iTRAQ ratios (IS to vehicle or PCS to vehicle) were first \log_2 transformed. After \log_2 ratio transformation, differentially expressed protein lists were created by identifying only proteins that possessed \log_2 -transformed iTRAQ ratios 2 SD ($P < 0.05$) from the calculated mean background expression variation level. Significant differentially expressed protein lists (comprising proteins elevated or reduced in their expression in response to IS or PCS) were then used for additional bioinformatics deconvolution using diverse informatics platforms, including Ingenuity Pathway Analysis (IPA; Canonical Signaling Pathway and Upstream Regulator applications; <https://www.qiagen-bioinformatics.com/products/ingenuity-pathway-analysis/>), GeneIndexer^{23,24} (<https://geneindexer.com/>), WebGestalt,²⁵ and VennPlex²⁶ (<https://www.irp.nia.nih.gov/bioinformatics/vennplex.html>).

Analyses of Molecular Gene Expression in the Aorta and Kidney

The mRNA transcript expression of glyceraldehyde-3-phosphate dehydrogenase (GAPDH; Rn99999916_s1) and GLUT1 (Rn01417099_m1) was determined in the distal part of the abdominal aorta. Total mRNA was extracted using the RNeasy Fibrous Tissue mini kit (Qiagen, Hilden, Germany) and reverse transcribed to cDNA by the High Capacity cDNA archive kit (Applied Biosystems, Foster City, CA). Real-time PCR with an ABI Prism 7000 Sequence Detection System (Applied Biosystems) on the basis of TaqMan fluorescence methodology was used for mRNA quantification. TaqMan probe and primers were purchased as TaqMan gene expression assays on demand from Applied Biosystems. Each gene was tested in triplicate and normalized to the expression of the housekeeping transcript GAPDH.

A similar experimental protocol was performed to investigate the mRNA transcript expression of GAPDH (Rn99999916_s1), IL-1 β (Rn00580432_m1), collagen I

(Rn00801649_g1), klotho (Rn00580123_m1), TGF- β (Rn00572010_m1), TNF- α (Rn00562055_m1), and vascular cell adhesion molecule 1 (Rn00563627_m1) in the left kidney.

Statistical Analyses

Statistical comparisons were made by nonparametric testing (SPSS 23.0 software; IBM Corp., Armonk, NY). To investigate the statistical difference between groups at one timepoint, a Kruskal–Wallis test followed by Mann–Whitney U test was applied. Comparisons between timepoints within each group were performed with a Friedman related samples test followed by a Wilcoxon signed rank test. Bonferroni correction was assessed when more than two groups were compared. To investigate the relationship between aortic calcification and biochemical parameters, a Spearman rho univariate correlation analysis was performed. Representative data are presented as mean \pm SEM and considered significant with a P value ≤ 0.05 .

RESULTS

Animal Study #1

IS or PCS Exposure Does Not Aggravate Chronic Renal Failure
Chronic renal failure, mimicking CKD, was effectively induced in our experimental cohorts via adenine dosing as evidenced by a significant increase in serum creatinine levels (Figure 1A) and a decline in creatinine clearance (Figure 1B). Vehicle-exposed CKD rats demonstrated an increase in serum phosphorus levels, reflecting a moderate state of hyperphosphatemia (Figure 1C) and a nonsignificant trend toward hypocalcemia (Figure 1D)—both characteristic facets of CKD. Comparable creatinine, phosphorus, and calcium values were also observed in CKD rats exposed to PCS. IS-exposed CKD rats exhibited significantly lower serum creatinine and phosphorous levels at weeks 5 and 7 as well as significantly higher serum calcium concentrations at weeks 3 and 7 compared with vehicle-exposed CKD rats (Figure 1, A, C, and D). Furthermore, alterations in calcium and phosphorus homeostasis were in line with a significant increase of serum PTH levels in CKD rats exposed to vehicle ($14,407 \pm 2283$ pg/ml; $P = 0.02$), IS (7932 ± 2432 pg/ml), and PCS ($10,923 \pm 3415$ pg/ml; $P = 0.03$) compared with historical control values of rats with normal renal function (938 ± 78 pg/ml). However, no differences in serum PTH levels between CKD rats exposed to vehicle, IS, or PCS were observed at the end of the study.

To rule out the possibility of the lower serum creatinine levels in the IS group being due to interference of the toxin with the adenine metabolism and thus, with the renal 2,8-dihydroxyadenine crystal formation, we also quantified the renal crystal content in our rats. Our results demonstrate no differences in the percentages of renal tissue area covered by 2,8-dihydroxyadenine crystals in CKD rats exposed to IS ($3.41\% \pm 0.31\%$), PCS ($2.97\% \pm 0.24\%$), or vehicle ($3.10\% \pm 0.15\%$).

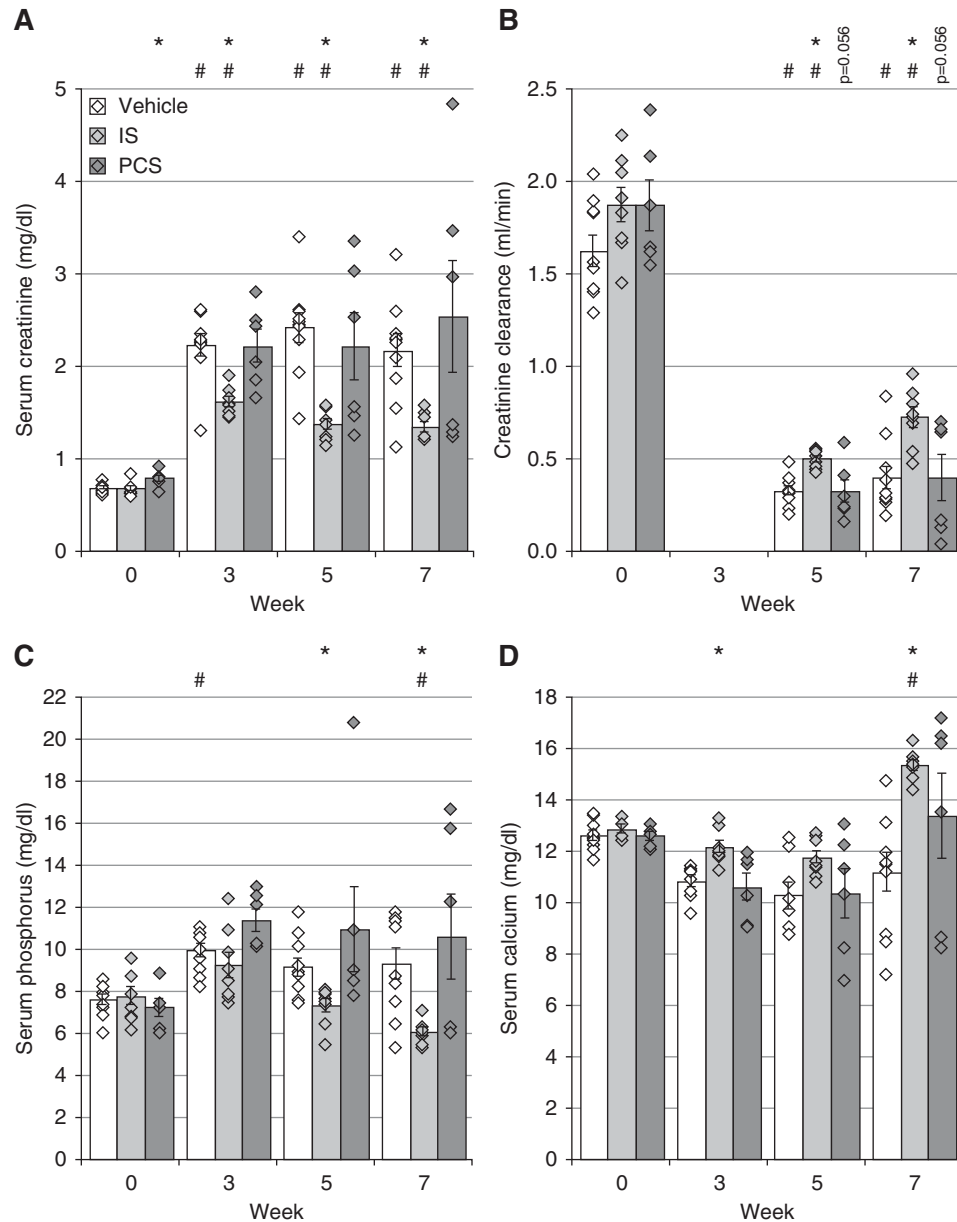


Figure 1. Indoxyl sulfate (IS) or p-cresyl sulfate (PCS) exposure does not aggravate chronic renal failure. (A) Serum creatinine, (B) creatinine clearance, (C) serum phosphorus, and (D) serum calcium levels. Data are presented as mean \pm SEM. * P <0.05 versus vehicle; # P <0.05 versus week 0.

IS and PCS Exposure Does Not Deteriorate Renal Fibrosis and Inflammation

To investigate whether exposure to uremic toxins modulates renal fibrosis and inflammation, a characteristic feature of adenine-induced CKD, mRNA expression profiles of inflammatory and fibrotic markers were studied in the kidney. Although a trend toward lower mRNA expression of the inflammatory genes IL-1 β , TNF- α , and vascular cell adhesion molecule 1 was detected in CKD rats exposed to IS or PCS compared with vehicle-exposed CKD rats, no significant differences between the study groups were found (Figure 2, A–C). Nevertheless, CKD rats exposed to IS demonstrated a

significantly decreased mRNA expression of the fibrosis markers collagen I and TGF- β compared with vehicle-exposed CKD rats (Figure 2, D and E). In addition, compared with vehicle-exposed CKD rats, no difference in *klotho* mRNA expression was observed for either IS- or PCS-exposed CKD rats (Figure 2F).

Time-Averaged Serum Concentrations of IS or PCS

On the basis of the IS and PCS serum levels at weeks 0, 3, 5, and 7, time-averaged concentrations of IS and PCS were calculated. CKD rats exposed to IS showed a significant increase in time-averaged concentration of IS ($69.4 \pm 5.7 \mu\text{M}$; P <0.001)

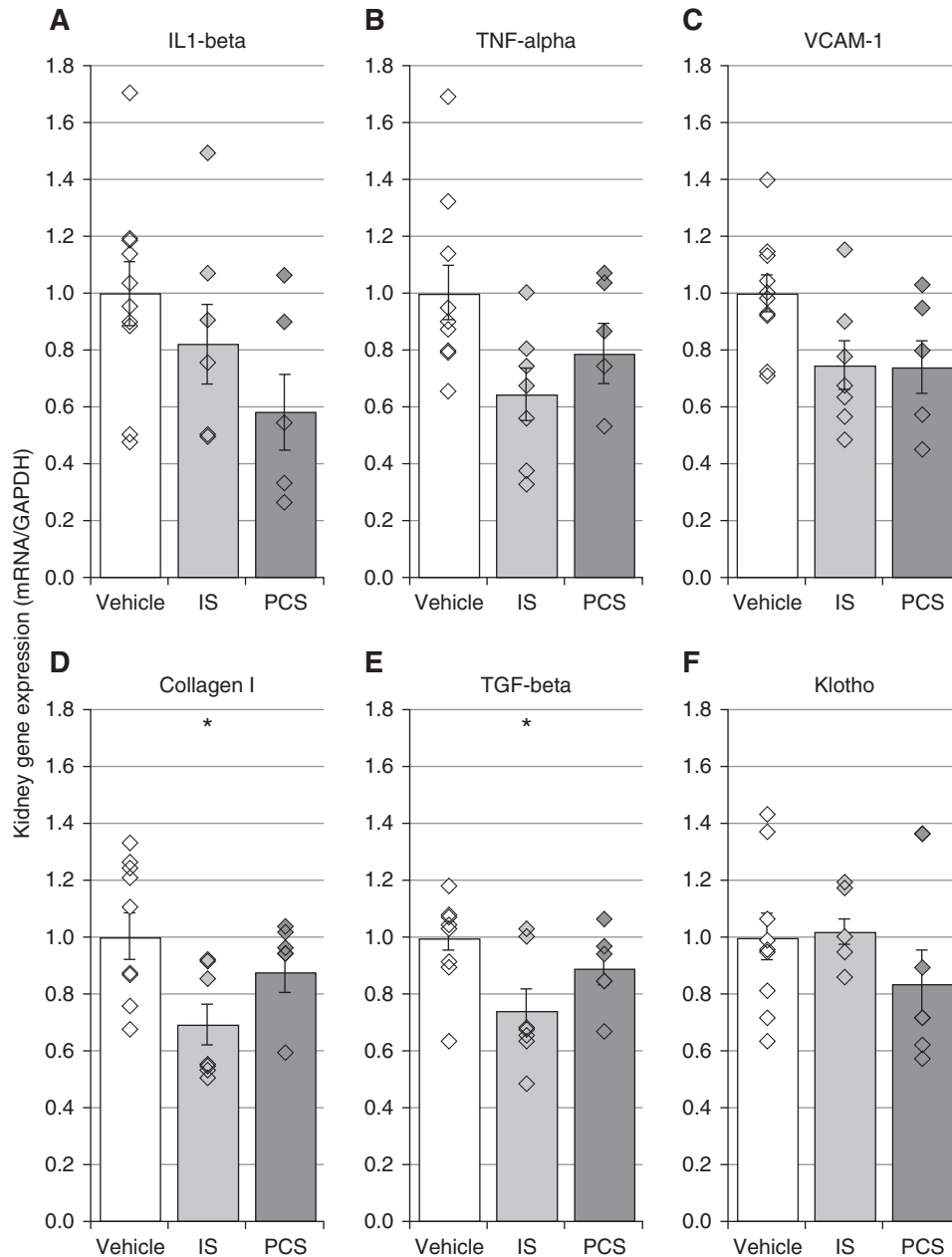


Figure 2. Indoxyl sulfate (IS) and p-cresyl sulfate (PCS) exposure does not deteriorate renal inflammation and fibrosis. Total mRNA expression of (A–C) inflammatory genes, (D and E) fibrosis-related genes, and (F) klotho gene in the kidney of IS- or PCS-exposed CKD rats versus vehicle-exposed CKD rats. Data are presented as mean±SEM. GAPDH, glyceraldehyde-3-phosphate dehydrogenase; VCAM-1, vascular cell adhesion molecule 1. **P*<0.05 versus vehicle.

compared with vehicle-exposed CKD rats ($35.3 \pm 3.6 \mu\text{M}$). Additionally, the time-averaged concentration of PCS was also significantly elevated in PCS-exposed CKD rats ($151.0 \pm 40.7 \mu\text{M}$; *P*=0.002) compared with vehicle-exposed CKD rats ($4.8 \pm 0.8 \mu\text{M}$).

IS and PCS Exposure Influences Glucose Metabolism

Because circulating glucose and altered insulin receptor (INSR) activities have been associated with vascular

calcification, the effect of both uremic toxins on the glucose metabolism was investigated. CKD rats demonstrated significantly increased serum glucose concentrations after 7 weeks of IS or PCS exposure, which was not the case in vehicle-exposed CKD rats (Figure 3A). Furthermore, CKD rats exposed to IS and PCS had a lower expression of GLUT1, a major glucose uptake transporter, in the aorta—this attenuation achieved significance in the PCS group (Figure 3B).

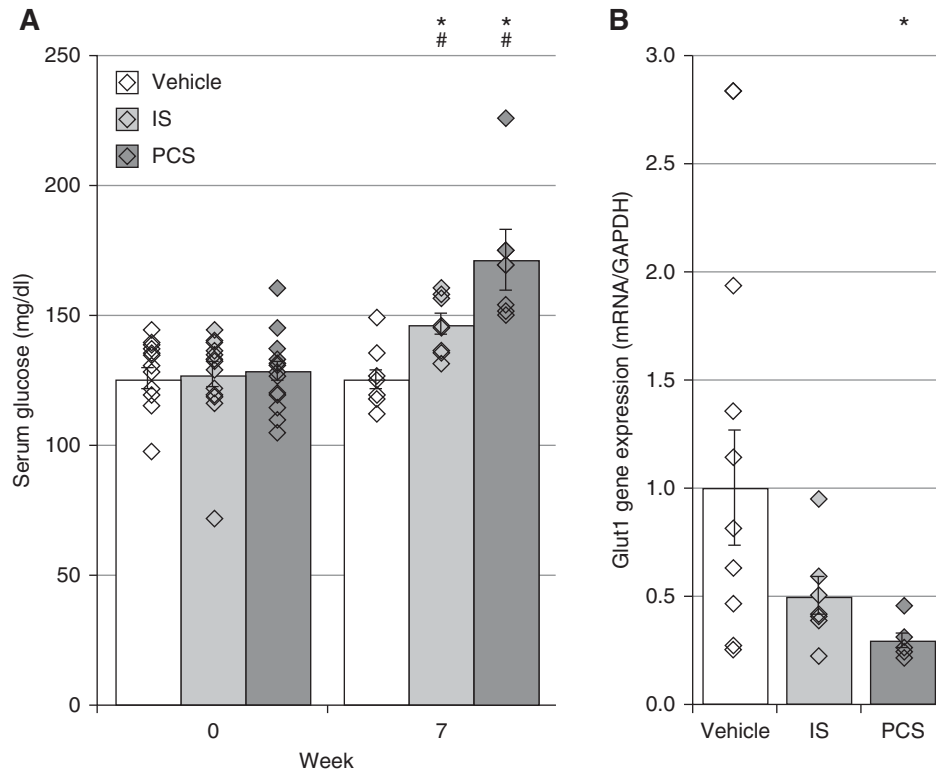


Figure 3. Indoxyl sulfate (IS) and p-cresyl sulfate (PCS) exposure elevate resting glucose and decrease glucose transporter 1 (GLUT1) transcript expression in the aorta. (A) Serum glucose levels and (B) mRNA expression of GLUT1 in vehicle-, IS-, and PCS-exposed rats. Data are presented as mean \pm SEM. GAPDH, glyceraldehyde-3-phosphate dehydrogenase. * P <0.05 versus vehicle; # P <0.05 versus week 0.

IS and PCS Promote Calcification in the Aorta and Peripheral Arteries

The effect of IS and PCS on vascular calcification in CKD rats was investigated by determining the calcium content in several arteries. Both IS and PCS exposure significantly augmented aortic calcification. Aortic calcium content in both IS- and PCS-exposed CKD rats was tenfold higher compared with vehicle-exposed ones (Figure 4A). Significant increases in calcium content were also observed in the carotid and femoral arteries of CKD rats exposed to IS and PCS (Figure 4, B and C). These results were reinforced by a distinct Von Kossa positivity on aortic cross-sections of IS- and PCS-exposed CKD rats. In line with the total calcium content, a significantly increased calcified tissue surface was found in CKD rats exposed to the uremic toxins (Figure 4D). Von Kossa staining also revealed that calcifications were uniquely located in the medial layer of the aortic wall (Figure 4E). Aortic calcification was significantly correlated with serum calcium (week 5: $r=0.48$; $P<0.05$ and week 7: $r=0.65$; $P<0.01$), serum IS (week 3: $r=0.61$; $P<0.01$), serum PCS (week 3: $r=0.52$; $P<0.05$ and week 5: $r=0.64$; $P<0.01$), and serum glucose (week 7: $r=0.52$; $P<0.01$).

IS and PCS Do Not Disturb Static and Dynamic Bone Parameters

As in CKD, the development of vascular calcification has been associated with a disturbed bone metabolism (*i.e.*, the bone-vascular axis),²⁷ and we investigated whether exposure to IS or

PCS also affected bone histology. Table 1 represents the measured values of the static and dynamic bone parameters of CKD rats exposed to vehicle, IS, or PCS. As evidenced from various previous reports,^{28–30} adenine-induced CKD in the rat goes along with the development of high-bone turnover disease as indicated by increased osteoid, eroded zones, and elevated osteoblast as well as osteoclast numbers. In this study, CKD rats exposed to vehicle and PCS displayed similar values of all static bone parameters under study. Compared with the vehicle CKD group, IS-exposed CKD rats showed significantly lower levels of the osteoid perimeter, osteoid width, and osteoblast perimeter, which were similar to those observed in bone of rats with normal kidney function (historical data). Dynamic bone parameters, (*i.e.*, bone formation rate and mineralization apposition rate) did not differ significantly between the study groups.

IS- and PCS-Induced Calcification Associates with Activation of Inflammation and Coagulation Pathways in the Aorta

To comprehensively study the molecular signaling behavior associated with toxin-mediated arterial calcification in the setting of CKD, we decided to use relative quantitative proteomic analysis of aortas extracted from IS- and PCS-exposed CKD rats versus vehicle-exposed ones. Using stringent and significant cutoff criteria for protein identification (99% percentile peptide identification confidence) and significant deviation

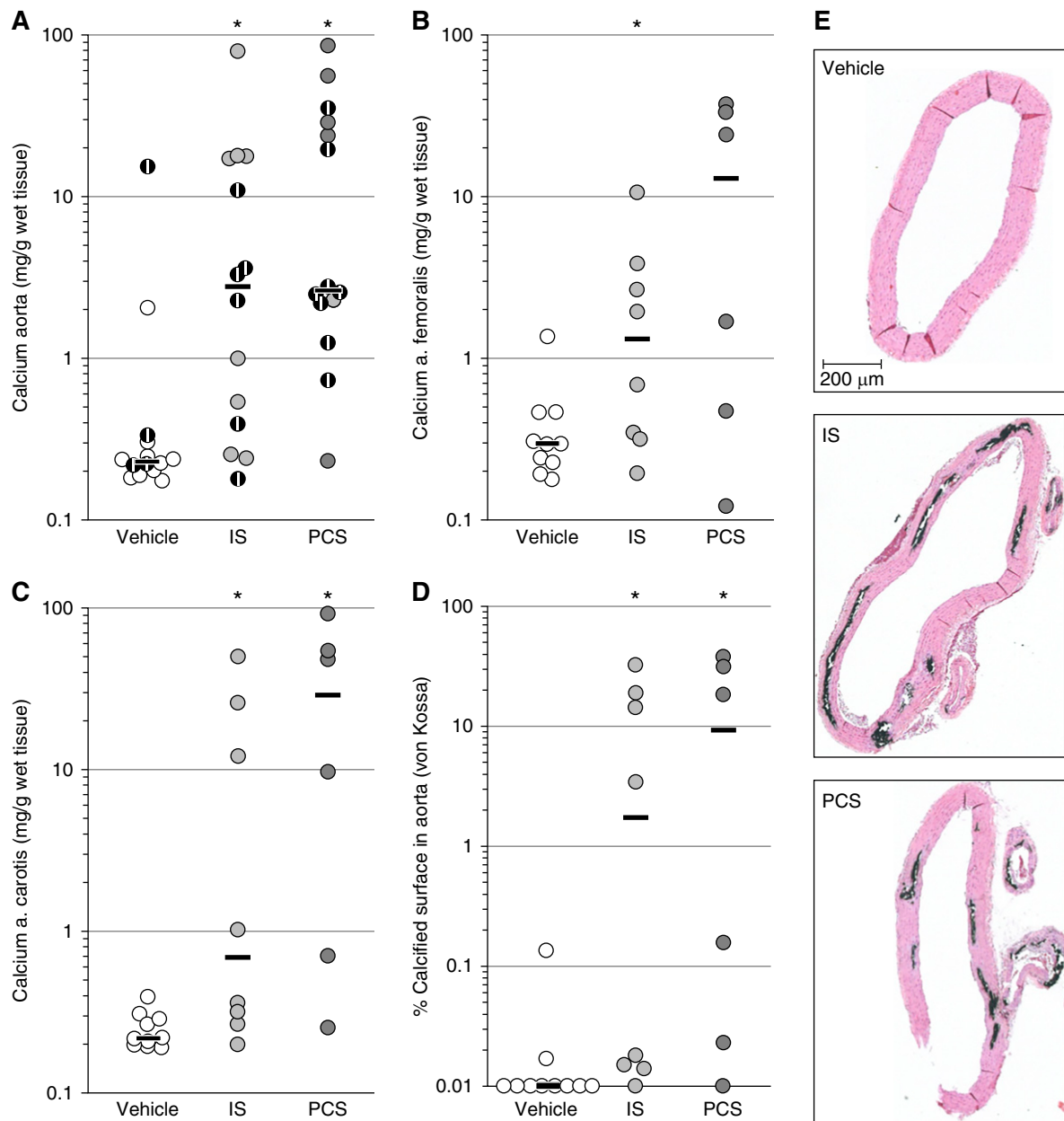


Figure 4. Indoxyl sulfate (IS) and p-cresyl sulfate (PCS) promote calcification in the aorta and peripheral arteries. Calcium contents of the (A) aorta, (B) femoral artery, and (C) carotid artery and (D) the percentage of calcified aortic area of CKD rats exposed to vehicle, IS, or PCS. Black dots with a white stripe represent rats that died before the planned euthanasia. Black bars represent the median. * $P \leq 0.05$ versus vehicle. (E) Visualization of calcification in aortic sections. Representative Von Kossa–stained aortic sections of a vehicle-, IS-, and PCS-exposed CKD rat. Magnification, $\times 62.5$.

from the expression background (95% percentile deviation from control levels in control animals), we found that IS and PCS exposure resulted in a significant alteration of 268 (120 upregulated and 148 downregulated) (Supplemental Table 1) and 262 (115 upregulated and 147 downregulated) (Supplemental Table 2) proteins, respectively (Figure 5A). At a simple protein identity level, the proteomic expression responses in aortic tissue were highly similar between IS and PCS (Figure 5A) (38% of the proteins were common; *i.e.*,

203 of 530 proteins were common between IS and PCS), and we further investigated the global similarities at the proteomic level in IS- and PCS-exposed aortic tissues with quantitative Venn diagram analyses. The ten most upregulated or downregulated proteins that were common between IS- or PCS-exposed rat aortic samples are presented in Supplemental Table 3.

WebGestalt-based gene ontology (GO) biologic process analysis of the common IS/PCS proteomic responses was

Table 1. Static and dynamic bone parameters of CKD rats exposed to vehicle, indoxyl sulfate, or p-cresyl sulfate

Bone Parameters	Vehicle	IS	PCS	Reference Values of Rats with Normal Renal Function
Static bone parameters				
Bone area (% of tissue area)	31.4±2.4	24.9±3.8	36.1±6.1	24.41±2.0
Mineralized area (% of tissue area)	29.8±2.4	24.1±3.6	34.4±5.9	23.28±1.88
Osteoid perimeter (% of total perimeter)	34.8±3.1	23.1±2.4 ^a	30.2±3.9	27.46±8.24
Eroded perimeter (% of total perimeter)	10.8±1.0	9.3±1.4	14.0±2.4	10.26±0.75
Osteoid width (μm)	6.26±0.4	4.72±0.28 ^a	6.71±0.6	5.38±0.74
Osteoblast perimeter (% of total perimeter)	25.6±3.0	13.8±2.4 ^a	21.4±3.1	11.3±3.7
Osteoclast perimeter (% of total perimeter)	3.7±0.5	3.0±0.5	4.2±0.6	3.56±0.51
Dynamic bone parameters				
Bone formation rate (μm ² /mm ² per day)	5602±528	4558±971	3445±997	1994±213
Mineralization apposition rate (μm/d)	4.73±0.19	4.59±0.42	4.59±0.66	2.55±0.19

Data are presented as mean±SEM. IS, indoxyl sulfate; PCS, p-cresyl sulfate.

^aP<0.05 versus vehicle.

performed to link and coherently cluster these proteins to simple biologic processes. The 203 proteins common to both significantly regulated IS and PCS datasets (Figure 5A) populated (at a $P<0.05$ significance level) the following biologic processes: “Acute Phase Response,” “Iso-Citrate Metabolic Process,” and “Complement Activation” (Figure 5B). In addition to GO-based biologic process clustering, we also used signaling pathway analysis (IPA-based canonical signaling pathway analysis) to generate an orthogonal and more mechanistic signaling appreciation of our IS/PCS common dataset (Supplemental Table 4). In accordance with our GO term clustering, we found that “Acute Phase Signaling” was prominent in the signaling pathways, which were significantly populated by proteins from the common IS/PCS dataset (Figure 5C). The “Acute Phase Signaling” pathway was populated predominantly by upregulated proteins from the common IS/PCS dataset, suggesting that uremic toxin exposure induces a potent stimulation of this signaling pathway. Several of the other common IS/PCS dataset significantly populated and positively stimulated pathways were associated with procoagulative activity (“Intrinsic/Extrinsic Prothrombin Activation Pathways” and “Coagulation System”) (Figure 5C). The common signaling pathways strongly populated in an inhibitory manner (*i.e.*, largely populated by downregulated proteins) by the IS/PCS-exposed datasets were consistently associated with stress responsiveness (“Glutathione Mediated Detoxification,” “Glutathione Redox Reactions I,” and “Glucocorticoid Receptor Signaling”), metabolic activity (“Fatty Acid β -Oxidation I” and “TCA Cycle II”), and calcium-associated processes (“Calcium Signaling”) (Figure 5C).

To supplement both our GO biologic process clustering and signaling pathway analysis, we used perturbagen response pattern matching (using the IPA-based “Upstream Analysis” suite) between our IS/PCS differential expression dataset (203 proteins) and IPA-curated perturbagen (chemical or genetic/proteomic) response patterns. This analysis aims to identify upstream regulators that are responsible for the up- or down-regulation of common IS/PCS proteins by assessing the degree of

overlap (at both the protein identity and expression polarity levels) between our input IS/PCS common dataset and multiple curated perturbagen datasets. Both upstream chemical factors and protein/genetic factors linked to our common IS/PCS proteome dataset revealed a consistent and strong role for altered energy metabolism coincident with the IS/PCS-induced calcification process, including elevated glucose levels and impaired insulin signaling/sensitivity as indicated by reduced INSR as well as peroxisome proliferation-activated receptor- α (PPAR α) and PPAR γ expression (Figure 6A).

Almost all IS- and PCS-exposed CKD animals developed significant aortic calcifications. Each group, however, contained one or two animals that failed to demonstrate calcifications (*i.e.*, “escapees” from the procalcifying effects of the uremic toxins). To investigate this potential pathologic escape mechanism from vascular calcification, we compared the multiple protein expression pattern differences between vehicle-exposed CKD rats and noncalcified IS/PCS-exposed CKD rats using our iTRAQ proteomic platform. In “noncalcified” IS- and PCS-exposed aortic samples, 183 proteins (109 upregulated and 74 downregulated) (Supplemental Table 5) and 232 proteins (132 upregulated and 100 downregulated) (Supplemental Table 6), respectively, were significantly altered compared with vehicle. Interestingly, in contrast to the “calcified” IS/PCS proteome (Supplemental Tables 1 and 2), IS- and PCS-exposed CKD rats that did not develop calcifications in the aortic wall showed no significant activation in the previously mentioned “procalcifying” pathways, including “Acute Phase Response,” “Intrinsic Prothrombin Activation,” and “Coagulation System.” In contrast, however, a significant activation of the farnesoid/liver X-retinoid X receptor functionality pathway (“LXR/FXR-RXR Activation” [lipid metabolism]) was predicted (Figure 6B). Differential pathway analysis thus demonstrated that, with respect to the strength of pathway enrichment, the “Acute Phase Response,” “Intrinsic Prothrombin Activation,” and “Coagulation System” pathways promoted calcification, whereas LXR/RXR antagonized vascular calcification. Likewise, we found that the predicted

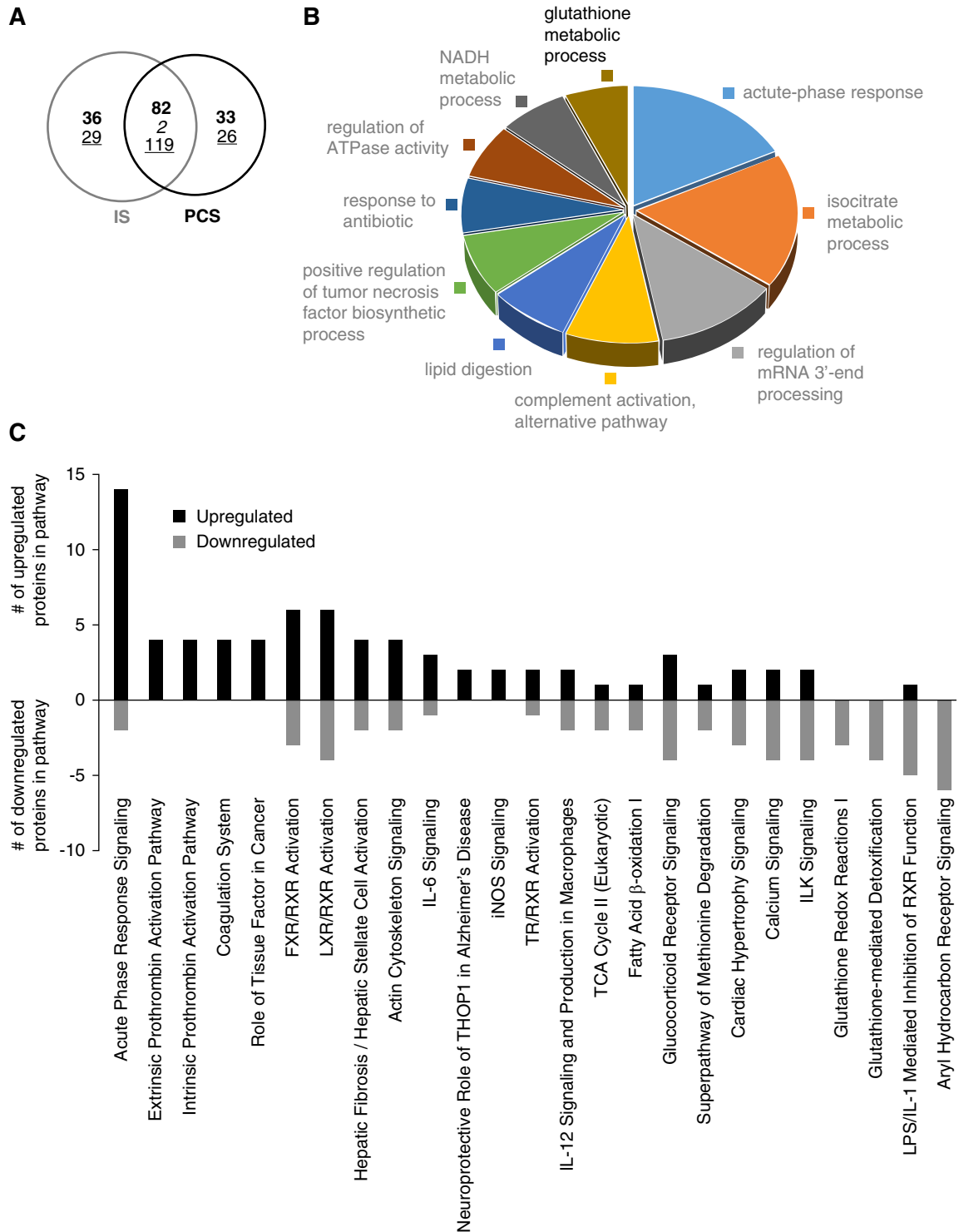


Figure 5. Indoxyl sulfate (IS)/p-cresyl sulfate (PCS) induced aortic calcification associates with activation of inflammation and coagulation pathways in the aorta. (A) Quantitative Venn diagram analysis of the global similarities at the proteomic level in IS- and PCS-exposed aortic tissues versus vehicles. The intersection between both circles shows the number of proteins that are common between IS- and PCS-exposed CKD rats. Bold and underlined numbers represent upregulated and downregulated proteins, respectively. The number indicated in italics represents the number of proteins that were contraregulated between IS- and PCS-exposed aortic samples. (B) Gene ontology and (C) ingenuity pathway analysis of the common IS/PCS proteome with the number of upregulated (black bars) or downregulated (gray bars) proteins in each pathway.

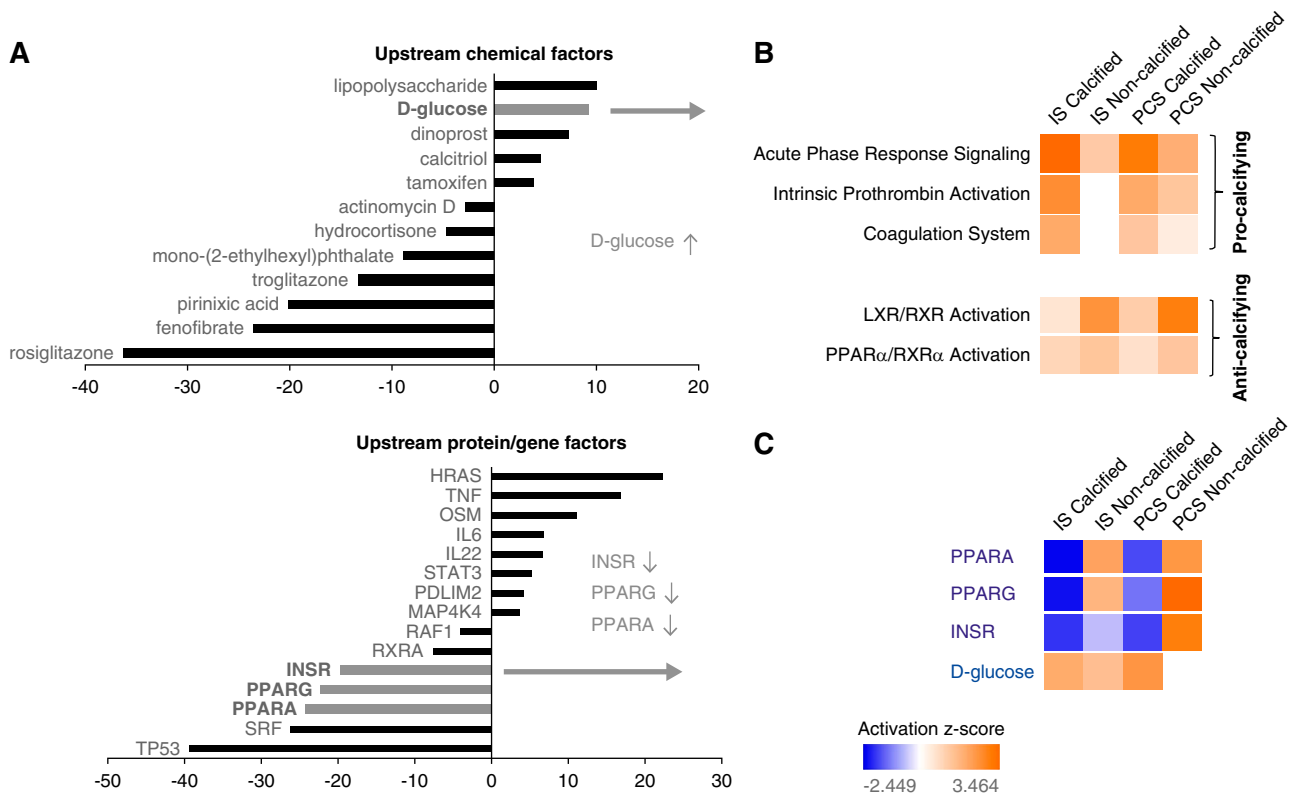


Figure 6. Inflammation, coagulation and glucometabolism pathways strongly associate with indoxyl sulfate (IS)/p-cresyl sulfate (PCS) induced calcification while escape from toxin-induced calcification was linked with liver X receptors and farnesoid X/liver X receptor signaling pathways. (A) Identification of the upstream chemical and protein/gene factors that are responsible for the up- or down-regulation of genes in the common IS/PCS proteome was performed. Ingenuity Pathway Analysis ascribes a quantified z-score number (ordinate axis) that determines whether an upstream regulator has significantly more “activated” predictions ($z > 0$) than “inhibited” predictions ($z < 0$). A consistent and strong role for altered energy metabolism was observed, including elevated glucose levels (gray bar in upper panel) as well as decreased insulin receptor (INSR) function and peroxisome proliferation-activated receptor (PPAR) activity (gray bars in lower panel). The upregulation (orange) and downregulation (blue) of (B) the signaling pathways “Acute Phase Response Signaling,” “Intrinsic Prothrombin Activation,” “Coagulation System,” and “LXR/RXR Activation (Lipid Metabolism)” and (C) upstream proteomic perturbagens “PPAR α ,” “PPAR γ ,” “Insulin Receptor (INSR),” and “D-Glucose” in IS- and PCS-exposed CKD rats with or without aortic calcification.

effects on upstream proteome regulation (using the IPA-based “Upstream Analysis” suite) were highly divergent between calcified and noncalcified IS- and PCS-exposed CKD rats. Although aortic calcification was strongly linked with downregulation of INSR and PPAR activity and elevated glucose levels, noncalcified IS/PCS vessels were associated with an opposing degree of INSR and glucose modulation (Figure 6C).

Animal Study #2

To further investigate whether the induction of inflammation and coagulation pathways in the aorta is directly caused by these uremic toxins and is not just the consequence of the calcification process in the vessel wall itself, we additionally studied the changes in molecular signaling pathways during the induction phase (*i.e.*, before arterial injury and calcification is well established). CKD rats exposed to vehicle, IS, or PCS for 4 days showed an equally fourfold increase in serum creatinine values after 4 days of CKD induction (Supplemental Table 7).

CKD rats exposed to IS had significantly elevated serum IS levels, whereas those exposed to PCS showed significantly higher serum PCS values (Supplemental Table 7). No calcification in the aorta was observed after 4 days of vehicle or toxin exposure in CKD rats exposed to IS (0.11 ± 0.01 mg Ca/g tissue), PCS (0.14 ± 0.08 mg Ca/g tissue), or vehicle (0.08 ± 0.01 mg Ca/g tissue) as evidenced by the very low aortic calcium levels, which are in the range of values from control rats with normal renal function.²⁷ Relative quantitative proteomic analysis of aortas extracted from IS- and PCS-exposed CKD rats versus vehicle-exposed ones followed by canonical signaling pathway analysis revealed that the “Acute Phase Response Signaling Pathway,” “Intrinsic/Extrinsic Prothrombin Activation Pathways,” and “Coagulation System” are predominantly activated in the aorta of CKD rats after short-term exposure of IS or PCS (Figure 7), which corresponds very well with the outcome of the proteomic analysis after long-term exposure to these toxins as described in animal study #1. Remarkably,

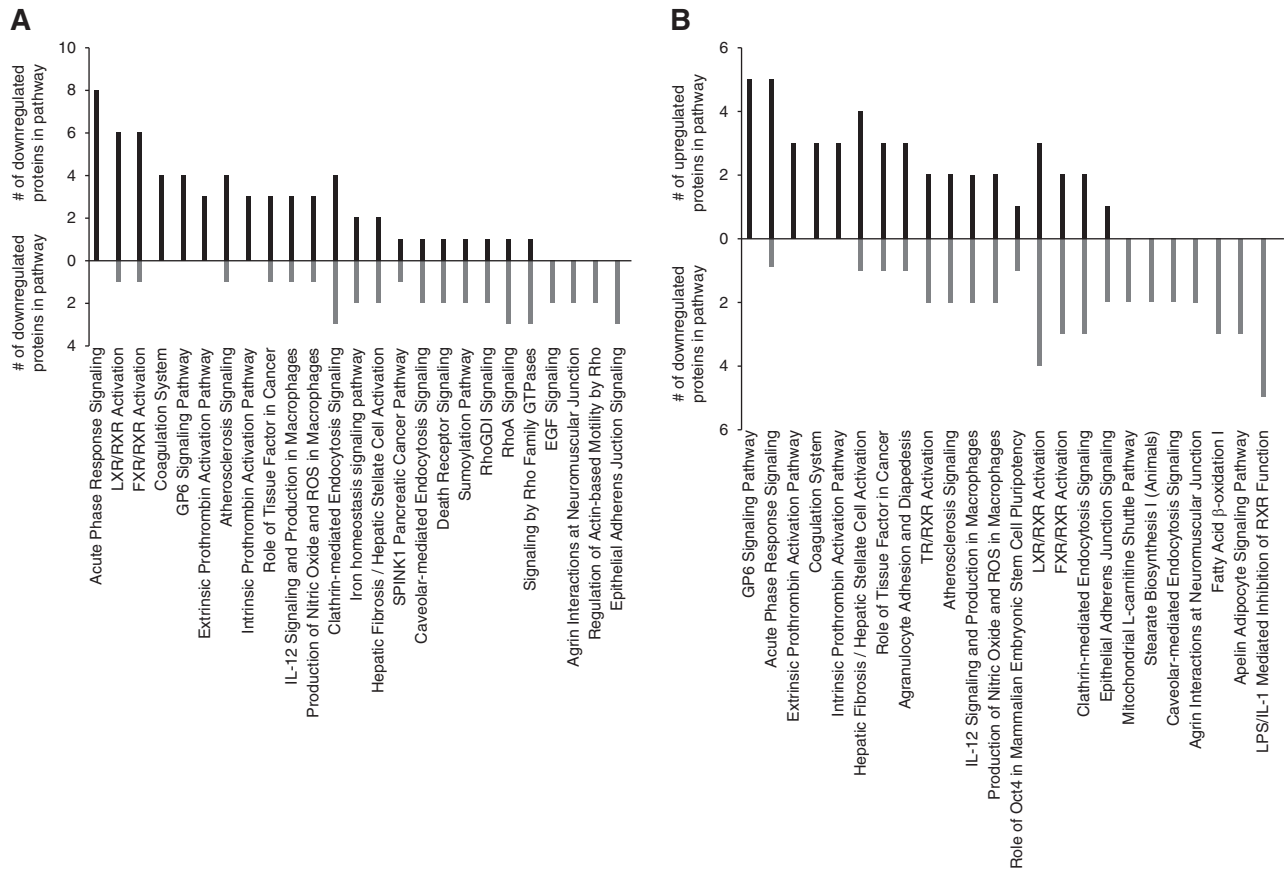


Figure 7. Short-term indoxyl sulfate (IS) and p-cresyl sulfate (PCS) exposure generates a functional signature reminiscent of long-term uremic toxin exposure. Ingenuity canonical signaling pathway analysis (top 25 most significantly populated pathways) with the number of upregulated (black bars) or downregulated (gray bars) proteins in each pathway after short-term exposure of (A) IS and (B) PCS in CKD rats.

glycoprotein 6 (GP6) signaling popped up after short-term IS and PCS exposure (Figure 7). GP6 is a platelet membrane receptor involved in platelet activation.

DISCUSSION

There is substantial evidence supporting the hypothesis that the uremic toxins IS and PCS are related to cardiovascular mortality.^{5,31,32} However, no direct *in vivo* evidence for a causal role of these toxins in the pathology of CKD-related vascular calcification has been reported so far. In this study, we demonstrate that IS and PCS promote calcification in the aorta and peripheral vessels in rats with adenine-induced CKD.

Adenine dosing of rats led to the typical clinical picture of CKD evidenced by decreased creatinine clearance as well as altered mineral homeostasis characterized by abnormal levels of phosphorus, calcium, and PTH and a disturbed bone metabolism. However, with the adenine dosing strategy applied in this study, development of significant vascular calcification

could deliberately be restricted to only 2 of 14 vehicle-exposed CKD rats. CKD rats exposed to either IS or PCS, however, distinctly and significantly promoted the development of moderate to severe arterial calcifications, which implicates a direct role for both toxins as inducers of vascular calcification in the arteries of CKD rats. These effects were seen at serum IS and PCS levels comparable with the reported serum IS (104.7 [67.2–134.6] μM) and PCS (183.6 [114.4–305.3] μM) values in patients on hemodialysis.³³

Because the development and progress of vascular calcification greatly depend on the severity of renal failure² and/or a disordered bone metabolism either going or not going along herewith,²⁷ we investigated the possibility for the effect of IS or PCS on vascular calcification to be due to a direct effect of these compounds on renal function and bone metabolism. The literature has demonstrated that IS and PCS stimulate the progression of renal failure by increasing the inflammation in the proximal tubular cells and enhancing kidney fibrosis.^{34,35} Moreover, Sun *et al.*³⁶ suggested that IS and PCS suppress renal *klotho* expression through epigenetic

modifications. Several studies have considered *klotho* as a renoprotective factor, because reduced expression of this protein has been associated with increased kidney damage.^{37,38} Conversely, results of this study demonstrate that exposure to IS and PCS did not aggravate renal impairment, inflammation, and fibrosis in CKD rats, and it did not worsen serum biochemistry in terms of creatinine, phosphorus, and calcium levels in comparison with CKD rats exposed to vehicle. In addition, no significant differences in *klotho* expression for either IS- or PCS-exposed CKD rats versus those exposed to vehicle were observed.

Furthermore, other research groups have suggested that IS and PCS may also contribute to bone impairment by increasing reactive oxygen species in osteoblasts.^{39,40} However, we found that exposure to PCS did not alter static and dynamic bone parameters compared with vehicle exposure in CKD animals. Exposure to IS showed that all static bone parameters evolve toward values observed in the bone of rats with normal function, which was most probably due to the more preserved kidney function and smaller alterations in calcium and phosphorus homeostasis in this study group. Taken together, both IS and PCS exposure did not aggravate CKD, and it did not further disturb bone metabolism, which strongly suggests that both uremic toxins trigger the development/progression of moderate to severe vascular calcifications by direct deleterious effects on the vessel wall.

To investigate whether IS and PCS directly affect the arterial wall and to identify the molecular mechanisms and cellular signaling pathways by which these toxins exert their harmful effect on the vasculature, an unbiased quantitative proteomic approach using iTRAQ protein labeling and MS was applied. This methodology allowed us to simultaneously identify and quantify the proteins (in a high-dimensionality manner) that are differentially up- or downregulated in aortic samples of CKD rats exposed to IS and PCS versus those exposed to vehicle. Because the proteomic expression responses in arterial tissue were highly similar between IS and PCS versus vehicle condition, we focused on the common IS and PCS functional signature. By using functional annotation analysis of the common IS/PCS proteome, the following pathways were identified as being significantly activated by both toxins in aortic tissue samples: (1) the “Acute Phase Response Signaling” pathway (inflammation) and (2) the “Intrinsic and Extrinsic Prothrombin Activation” pathway (coagulation). Activation of inflammation and coagulation pathways coincided with calcification in the aorta after long-term exposure of IS and PCS, which makes it difficult to conclude whether these molecular changes are causally implicated in toxin-induced vascular calcification. An additional study showed that the “Acute Phase Response Signaling Pathway,” “Prothrombin Activation Pathways,” and “Coagulation System” are also predominantly activated after short-term exposure to IS or PCS and before calcification had developed. These findings thus correspond well with the molecular signaling pathways that are involved after long-term exposure to these toxins. They further illustrate that acute-phase response signaling and coagulation

signaling play a crucial causal role in the onset and development of toxin-induced vascular calcification. This is even more emphasized by the activation of GP6 signaling in aortas after short-term exposure to IS and PCS. GP6 indeed is the primary receptor for platelet/collagen interactions and subsequent platelet activation. Activation of this GP6 pathway in short-term toxin-exposed aortas that did not yet develop calcifications strongly suggests that platelet activation is initially involved in this toxin-mediated calcification process.

Interestingly, our experimental findings are in accordance with those observed in patients suffering from calcific aortic stenosis.⁴¹ In these patients, an integrated proteomic approach of serum samples indeed showed significant alterations in coagulation, inflammation, oxidative stress, and lipid metabolism. Activation of these signaling pathways plays a key role in the process of arterial calcification.

Subsequently, curated chemical and genomic/proteomic perturbagen matching analysis—predicting upstream regulators that could be responsible for the observed changes in the arterial proteins linked to inflammation and coagulation signaling pathways—revealed a major role for altered energy and glucose metabolism, including elevated glucose levels, INSR dysfunction, and impaired PPAR α and PPAR γ function. PPAR, particularly the PPAR γ isoform, is an important regulator of glucose metabolism, because activation of this nuclear receptor in adipocytes modulates the insulin signaling cascade, which improves insulin sensitivity.⁴² Interestingly, IS- and PCS-exposed CKD rats showed significantly altered vascular GLUT1 expression and significantly increased serum glucose levels, which were also significantly correlated with the calcium content in the aorta. These results strongly support our hypothesis that activation of inflammation and coagulation pathways by both uremic toxins is highly linked with increased circulating glucose levels and insulin resistance, which ultimately contribute to calcification of the arteries. Similar findings were reported by Koppe *et al.*,⁴³ who found that chronic PCS administration promoted insulin resistance and hyperglycemia in CKD mice. Systemic inflammation has been reported to enhance vascular calcification,^{44,45} whereas proinflammatory cytokines were found to induce a phenotypic switch of vascular cells into bone-like cells by which matrix vesicles containing hydroxyapatite are released into the vessel wall.^{46,47} Coagulation and inflammation are closely linked processes, because coagulation factors (fibrinogens and prothrombin) are also members of the acute-phase proteins.⁴⁸ Both “Intrinsic and Extrinsic Prothrombin Activation” pathways were significantly activated in calcified aortas of IS- and PCS-exposed CKD animals. Interestingly, vascular smooth muscle cells exposed to uremic serum have been reported to induce a significantly increased clot formation.⁴⁹ Other studies have also associated high-serum IS levels with thrombotic complications in patients with CKD.^{50,51} Furthermore, Kapustin *et al.*⁵² found that vascular smooth muscle cell exosomes, recently recognized as important mediators of calcification and coagulation,⁵³ are loaded with coagulation factors,

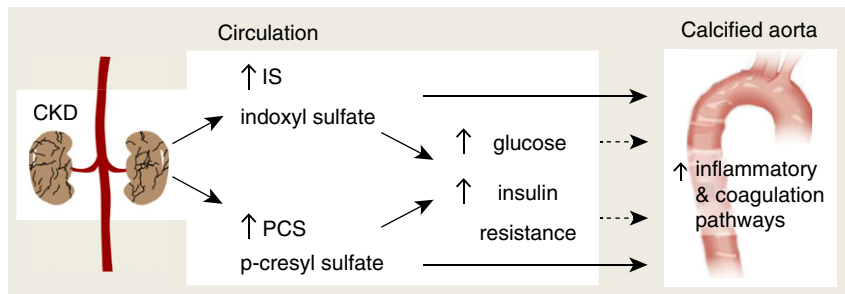


Figure 8. Mechanisms and pathways central to vascular calcification induced by indoxyl sulfate (IS) and p-cresyl sulfate (PCS).

such as prothrombin. Prothrombin accumulates in calcified human vessels, and a negative correlation between plasma prothrombin levels and vascular calcification has been reported.⁵² *In vitro* studies have also revealed that prothrombin inhibits vascular smooth muscle calcification,⁵² suggesting that, in our study, increased prothrombin acted as an inadequate defense mechanism. In addition, several clinical studies have associated coagulation with elevated coronary artery calcification scores.^{54,55} It is clear, therefore, that a close association between coagulation and vascular calcification exists, which opens a new research avenue for the identification of novel druggable targets.

Although IS and PCS exposure to CKD rats resulted in moderate to severe vascular calcification in the majority of the animals, some IS- and PCS-exposed rats failed to demonstrate significant arterial calcifications. To investigate a possible escape mechanism from calcifications in the arterial wall, a comparison between the aortic proteome profiles of noncalcified and calcified IS/PCS animals was performed. Interestingly, it was clear that, with respect to the strength (degree of enrichment probability and IPA-generated pathway z score) of pathway enrichment, the “Acute Phase Response,” “Intrinsic Prothrombin Activation,” and “Coagulation System” pathways promoted calcification, whereas “LXR/RXR (Lipid Metabolism)” pathways antagonized arterial calcification. The latter finding is supported by a study by Miyazaki-Anzai *et al.*⁵⁶ that reported that activation of FXR by a synthetic FXR agonist prevented the mineralization of bovine-calcifying vascular cells and inhibited vascular calcification in ApoE^{-/-} mice with CKD. Hence, it seems that procoagulation and inflammatory processes seem to be strongly linked with calcification events, whereas escape from these is rather associated with lipid metabolic functions. Moreover, with respect to predicted upstream proteome perturbagens responsible for the vascular proteomes, we found that, although calcification was associated with high glucose levels and downregulation of INSR activity, escape from vascular calcification was linked with an opposing degree of glucose and INSR modulation. Taken together, this further supports our hypothesis that IS and PCS promote calcification in the aorta and peripheral arteries of CKD rats *via* the induction of hyperglycemia and insulin resistance, which contribute to activation of the acute-phase response signaling and coagulation pathways in the arterial wall (Figure 8).

In conclusion, both protein-bound uremic toxins, IS and PCS, must be considered as important harmful vascular toxins and promoters of insulin resistance in CKD. Dietary interventions, such as probiotics to lower gut-derived uremic toxins, should be considered as a promising treatment for CKD-related vascular calcification. Identification of specific therapeutic targets in the molecular signaling pathways underlying the calcification process (*e.g.*, antidiabetic interventions, such as PPAR modulators, or insulin sensitizers, such as

metformin) is an important step to establishing novel therapies aimed at preventing or slowing down the progression of this vascular pathology.

ACKNOWLEDGMENTS

We thank Geert Dams, Hilde Geryl, Ludwig Lamberts, Rita Marynissen, and Simonne Dauwe for their excellent technical assistance and Dirk De Weerdts for his help with the graphics.

E. Neven is a postdoctoral fellow of the Fund for Scientific Research–Flanders (FWO). B. Opdebeeck and A. De Maré are fellows of the FWO.

DISCLOSURES

None.

SUPPLEMENTAL MATERIAL

This article contains the following supplemental material online at <http://jasn.asnjournals.org/lookup/suppl/doi:10.1681/ASN.2018060609/-/DCSupplemental>.

Supplemental Table 1. Differentially up- or downregulated proteins in IS-exposed calcified versus vehicle-exposed noncalcified aortic samples.

Supplemental Table 2. Differentially up- or downregulated proteins in PCS-exposed calcified versus vehicle-exposed noncalcified aortic samples.

Supplemental Table 3. The top ten upregulated or downregulated proteins common to both IS- and PCS-exposed rat aortic samples.

Supplemental Table 4. The top 25 most significantly altered canonical signaling pathways in the common IS and PCS aortic proteome.

Supplemental Table 5. Differentially up- or downregulated proteins in IS-exposed noncalcified versus vehicle-exposed noncalcified aortic samples.

Supplemental Table 6. Differentially up- or downregulated proteins in PCS-exposed noncalcified versus vehicle-exposed noncalcified aortic samples.

Supplemental Table 7. Biochemical parameters of CKD rats exposed to vehicle, indoxyl sulfate, or p-cresyl sulfate for 4 days.

REFERENCES

- London GM, Guérin AP, Marchais SJ, Métivier F, Pannier B, Adda H: Arterial media calcification in end-stage renal disease: Impact on all-cause and cardiovascular mortality. *Nephrol Dial Transplant* 18: 1731–1740, 2003
- Goodman WG, Goldin J, Kuizon BD, Yoon C, Gales B, Sider D, et al.: Coronary-artery calcification in young adults with end-stage renal disease who are undergoing dialysis. *N Engl J Med* 342: 1478–1483, 2000
- Tölle M, Reshetnik A, Schuchardt M, Höhne M, van der Giet M: Arteriosclerosis and vascular calcification: Causes, clinical assessment and therapy. *Eur J Clin Invest* 45: 976–985, 2015
- Barreto FC, Barreto DV, Liabeuf S, Meert N, Glorieux G, Temmar M, et al.: European Uremic Toxin Work Group (EUTox): Serum indoxyl sulfate is associated with vascular disease and mortality in chronic kidney disease patients. *Clin J Am Soc Nephrol* 4: 1551–1558, 2009
- Chiu CA, Lu LF, Yu TH, Hung WC, Chung FM, Tsai IT, et al.: Increased levels of total P-Cresylsulphate and indoxyl sulphate are associated with coronary artery disease in patients with diabetic nephropathy. *Rev Diabet Stud* 7: 275–284, 2010
- Liabeuf S, Barreto DV, Barreto FC, Meert N, Glorieux G, Schepers E, et al.: European Uraemic Toxin Work Group (EUTox): Free p-cresylsulphate is a predictor of mortality in patients at different stages of chronic kidney disease. *Nephrol Dial Transplant* 25: 1183–1191, 2010
- Evenepoel P, Meijers BK, Bammens BR, Verbeke K: Uremic toxins originating from colonic microbial metabolism. *Kidney Int Suppl* 114: S12–S19, 2009
- Meijers BK, Evenepoel P: The gut-kidney axis: Indoxyl sulfate, p-cresyl sulfate and CKD progression. *Nephrol Dial Transplant* 26: 759–761, 2011
- Dou L, Bertrand E, Cerini C, Faure V, Sampol J, Vanholder R, et al.: The uremic solutes p-cresol and indoxyl sulfate inhibit endothelial proliferation and wound repair. *Kidney Int* 65: 442–451, 2004
- Meijers BK, Van Kerckhoven S, Verbeke K, Dehaen W, Vanrenterghem Y, Hoylaerts MF, et al.: The uremic retention solute p-cresyl sulfate and markers of endothelial damage. *Am J Kidney Dis* 54: 891–901, 2009
- Six I, Gross P, Rémond MC, Chillon JM, Poirot S, Drueke TB, et al.: Deleterious vascular effects of indoxyl sulfate and reversal by oral adsorbent AST-120. *Atherosclerosis* 243: 248–256, 2015
- Yamamoto H, Tsuruoka S, Ioka T, Ando H, Ito C, Akimoto T, et al.: Indoxyl sulfate stimulates proliferation of rat vascular smooth muscle cells. *Kidney Int* 69: 1780–1785, 2006
- Muteliefu G, Enomoto A, Jiang P, Takahashi M, Niwa T: Indoxyl sulphate induces oxidative stress and the expression of osteoblast-specific proteins in vascular smooth muscle cells. *Nephrol Dial Transplant* 24: 2051–2058, 2009
- Neven E, De Schutter TM, De Broe ME, D'Haese PC: Cell biological and physicochemical aspects of arterial calcification. *Kidney Int* 79: 1166–1177, 2011
- Adijiang A, Goto S, Uramoto S, Nishijima F, Niwa T: Indoxyl sulphate promotes aortic calcification with expression of osteoblast-specific proteins in hypertensive rats. *Nephrol Dial Transplant* 23: 1892–1901, 2008
- Fujii H, Nishijima F, Goto S, Sugano M, Yamato H, Kitazawa R, et al.: Oral charcoal adsorbent (AST-120) prevents progression of cardiac damage in chronic kidney disease through suppression of oxidative stress. *Nephrol Dial Transplant* 24: 2089–2095, 2009
- Niwa T: Role of indoxyl sulfate in the progression of chronic kidney disease and cardiovascular disease: Experimental and clinical effects of oral sorbent AST-120. *Ther Apher Dial* 15: 120–124, 2011
- Goto S, Kitamura K, Kono K, Nakai K, Fujii H, Nishi S: Association between AST-120 and abdominal aortic calcification in predialysis patients with chronic kidney disease. *Clin Exp Nephrol* 17: 365–371, 2013
- Shafi T, Sirich TL, Meyer TW, Hostetter TH, Plummer NS, Hwang S, et al.: Results of the HEMO Study suggest that p-cresol sulfate and indoxyl sulfate are not associated with cardiovascular outcomes. *Kidney Int* 92: 1484–1492, 2017
- Evenepoel P, Glorieux G, Meijers B: p-Cresol sulfate and indoxyl sulfate: Some clouds are gathering in the uremic toxin sky. *Kidney Int* 92: 1323–1324, 2017
- Dempster DW, Compston JE, Drezner MK, Glorieux FH, Kanis JA, Malluche H, et al.: Standardized nomenclature, symbols, and units for bone histomorphometry: a 2012 update of the report of the ASBMR Histomorphometry Nomenclature Committee. *J Bone Miner Res* 28: 2–17, 2013
- Perez-Riverol Y, Csordas A, Bai J, Bernal-Llinares M, Hewapathirana S, Kundu DJ, et al.: The PRIDE database and related tools and resources in 2019: Improving support for quantification data. *Nucleic Acids Res* 47: D442–D450, 2019
- Roy S, Heinrich K, Phan V, Berry MW, Homayouni R: Latent Semantic Indexing of PubMed abstracts for identification of transcription factor candidates from microarray derived gene sets. *BMC Bioinformatics* 12 [Suppl 10]: S19, 2011
- Chadwick W, Martin B, Chapter MC, Park SS, Wang L, Daimon CM, et al.: GIT2 acts as a potential keystone protein in functional hypothalamic networks associated with age-related phenotypic changes in rats. *PLoS One* 7: e36975, 2012
- Wang J, Duncan D, Shi Z, Zhang B: WEB-based GENE SeT Analysis toolkit (WebGestalt): Update 2013. *Nucleic Acids Res* 41: W77–W83, 2013
- Cai H, Chen H, Yi T, Daimon CM, Boyle JP, Peers C, et al.: VennPlex—a novel Venn diagram program for comparing and visualizing datasets with differentially regulated datapoints. *PLoS One* 8: e53388, 2013
- Persy V, D'Haese P: Vascular calcification and bone disease: The calcification paradox. *Trends Mol Med* 15: 405–416, 2009
- Neven E, Bashir-Dar R, Dams G, Behets GJ, Verhulst A, Elseviers M, et al.: Disturbances in bone largely predict aortic calcification in an alternative rat model developed to study both vascular and bone pathology in chronic kidney disease. *J Bone Miner Res* 30: 2313–2324, 2015
- Neven E, De Schutter TM, Dams G, Gundlach K, Stepan S, Büchel J, et al.: A magnesium based phosphate binder reduces vascular calcification without affecting bone in chronic renal failure rats. *PLoS One* 9: e107067, 2014
- Neven E, Dams G, Postnov A, Chen B, De Clerck N, De Broe ME, et al.: Adequate phosphate binding with lanthanum carbonate attenuates arterial calcification in chronic renal failure rats. *Nephrol Dial Transplant* 24: 1790–1799, 2009
- Meijers BK, Claes K, Bammens B, de Loo H, Viaene L, Verbeke K, et al.: p-Cresol and cardiovascular risk in mild-to-moderate kidney disease. *Clin J Am Soc Nephrol* 5: 1182–1189, 2010
- Lin CJ, Wu CJ, Pan CF, Chen YC, Sun FJ, Chen HH: Serum protein-bound uraemic toxins and clinical outcomes in haemodialysis patients. *Nephrol Dial Transplant* 25: 3693–3700, 2010
- Meijers BK, De Loo H, Bammens B, Verbeke K, Vanrenterghem Y, Evenepoel P: p-Cresyl sulfate and indoxyl sulfate in hemodialysis patients. *Clin J Am Soc Nephrol* 4: 1932–1938, 2009
- Watanabe H, Miyamoto Y, Honda D, Tanaka H, Wu Q, Endo M, et al.: p-Cresyl sulfate causes renal tubular cell damage by inducing oxidative stress by activation of NADPH oxidase. *Kidney Int* 83: 582–592, 2013
- Bolati D, Shimizu H, Higashiyama Y, Nishijima F, Niwa T: Indoxyl sulfate induces epithelial-to-mesenchymal transition in rat kidneys and human proximal tubular cells. *Am J Nephrol* 34: 318–323, 2011
- Sun CY, Chang SC, Wu MS: Suppression of Klotho expression by protein-bound uremic toxins is associated with increased DNA methyltransferase expression and DNA hypermethylation. *Kidney Int* 81: 640–650, 2012
- Sugiura H, Yoshida T, Shiohira S, Kohei J, Mitobe M, Kurosu H, et al.: Reduced Klotho expression level in kidney aggravates renal interstitial fibrosis. *Am J Physiol Renal Physiol* 302: F1252–F1264, 2012

38. Doi S, Zou Y, Togao O, Pastor JV, John GB, Wang L, et al.: Klotho inhibits transforming growth factor-beta1 (TGF-beta1) signaling and suppresses renal fibrosis and cancer metastasis in mice. *J Biol Chem* 286: 8655–8665, 2011
39. Tanaka H, Iwasaki Y, Yamato H, Mori Y, Komaba H, Watanabe H, et al.: p-Cresyl sulfate induces osteoblast dysfunction through activating JNK and p38 MAPK pathways. *Bone* 56: 347–354, 2013
40. Nii-Kono T, Iwasaki Y, Uchida M, Fujieda A, Hosokawa A, Motojima M, et al.: Indoxyl sulfate induces skeletal resistance to parathyroid hormone in cultured osteoblastic cells. *Kidney Int* 71: 738–743, 2007
41. Mourino-Alvarez L, Baldan-Martin M, Gonzalez-Calero L, Martinez-Laborde C, Sastre-Oliva T, Moreno-Luna R, et al.: Patients with calcific aortic stenosis exhibit systemic molecular evidence of ischemia, enhanced coagulation, oxidative stress and impaired cholesterol transport. *Int J Cardiol* 225: 99–106, 2016
42. Leonardini A, Laviola L, Perrini S, Natalicchio A, Giorgino F: Cross-talk between PPARgamma and insulin signaling and modulation of insulin sensitivity. *PPAR Res* 2009: 818945, 2009
43. Koppe L, Pillon NJ, Vella RE, Croze ML, Pelletier CC, Chambert S, et al.: p-Cresyl sulfate promotes insulin resistance associated with CKD. *J Am Soc Nephrol* 24: 88–99, 2013
44. Bessueille L, Magne D: Inflammation: A culprit for vascular calcification in atherosclerosis and diabetes. *Cell Mol Life Sci* 72: 2475–2489, 2015
45. Demer LL, Tintut Y: Inflammatory, metabolic, and genetic mechanisms of vascular calcification. *Arterioscler Thromb Vasc Biol* 34: 715–723, 2014
46. El Hussein D, Boulanger MC, Mahmut A, Bouchareb R, Laflamme MH, Fournier D, et al.: P2Y2 receptor represses IL-6 expression by valve interstitial cells through Akt: Implication for calcific aortic valve disease. *J Mol Cell Cardiol* 72: 146–156, 2014
47. Lee HL, Woo KM, Ryoo HM, Baek JH: Tumor necrosis factor-alpha increases alkaline phosphatase expression in vascular smooth muscle cells via MSX2 induction. *Biochem Biophys Res Commun* 391: 1087–1092, 2010
48. Gruys E, Toussaint MJ, Niewold TA, Koopmans SJ: Acute phase reaction and acute phase proteins. *J Zhejiang Univ Sci B* 6: 1045–1056, 2005
49. Chitalia VC, Shivanna S, Martorell J, Balcells M, Bosch I, Kolandaivelu K, et al.: Uremic serum and solutes increase post-vascular interventional thrombotic risk through altered stability of smooth muscle cell tissue factor. *Circulation* 127: 365–376, 2013
50. Wu CC, Hsieh MY, Hung SC, Kuo KL, Tsai TH, Lai CL, et al.: Serum indoxyl sulfate associates with postangioplasty thrombosis of dialysis grafts. *J Am Soc Nephrol* 27: 1254–1264, 2016
51. Yang K, Du C, Wang X, Li F, Xu Y, Wang S, et al.: Indoxyl sulfate induces platelet hyperactivity and contributes to chronic kidney disease-associated thrombosis in mice. *Blood* 129: 2667–2679, 2017
52. Kapustin AN, Schoppet M, Schurgers LJ, Reynolds JL, McNair R, Heiss A, et al.: Prothrombin loading of vascular smooth muscle cell-derived exosomes regulates coagulation and calcification. *Arterioscler Thromb Vasc Biol* 37: e22–e32, 2017
53. Kapustin AN, Shanahan CM: Emerging roles for vascular smooth muscle cell exosomes in calcification and coagulation. *J Physiol* 594: 2905–2914, 2016
54. Green D, Chan C, Kang J, Liu K, Schreiner P, Jenny NS, et al.: Longitudinal assessment of fibrinogen in relation to subclinical cardiovascular disease: The CARDIA study. *J Thromb Haemost* 8: 489–495, 2010
55. Borissoff JI, Joosen IA, Versteylen MO, Spronk HM, ten Cate H, Hofstra L: Accelerated in vivo thrombin formation independently predicts the presence and severity of CT angiographic coronary atherosclerosis. *JACC Cardiovasc Imaging* 5: 1201–1210, 2012
56. Miyazaki-Anzai S, Levi M, Kratzer A, Ting TC, Lewis LB, Miyazaki M: Farnesoid X receptor activation prevents the development of vascular calcification in ApoE^{-/-} mice with chronic kidney disease. *Circ Res* 106: 1807–1817, 2010